NON-DARCIAN EFFECT ON DOUBLE-DIFFUSIVE NATURAL CONVECTION INSIDE AN INCLINED SQUARE DUPUIT-DARCY POROUS CAVITY UNDER A MAGNETIC FIELD

by

Redha REBHI[a], Noureddine HADIDI[a*], and Rachid BENNACER[b]

[a] University of Medea, FT, MEL, Medea, Algeria
[b] LMT-ENS Cachan, Cachan Cedex, France

Original scientific paper
https://doi.org/10.2298/TSCI190117271R

This paper presents a numerical study of a double diffusive convection in an inclined square porous cavity filled with an electrically conducting binary mixture. The upper and bottom walls are maintained at a constant temperatures and concentrations whereas the left and right walls are assumed to be adiabatic and impermeable. A uniform and tilted magnetic field is applied at an angle, γ, about the horizontal, it is obvious that this is related to the orientation of the magnetic force that can help or oppose the buoyant force. The Dupuit-Darcy flow model, which includes effects of the inertial parameter, with the Boussinesq approximation, energy, and species transport equations are solved numerically using the classical finite difference method. Governing parameters of the problem under study are the thermal Rayleigh number, Hartmann number, Lewis number, the buoyancy ratio, inclination angle, and tilting angle of the magnetic field. The numerical results are reported on the contours of streamline, temperature, and concentration and for the average Nusselt and Sherwood numbers for various parametric conditions. It is demonstrated that both the inertial effect parameter and the magnetic field, have a strong influence on the strength of the natural convection heat and mass transfer within the porous layer.

Key words: *double diffusive convection, inclined porous cavity, inertia effect, magnetic field*

Introduction

Double diffusive natural convection in porous enclosures is relevant to a wide range of industrial processes or environmental situations such as oceanography, astrophysics, geology, biology, chemical vapor transformation processes, solar power collectors, furnaces, building heating, and cooling systems, heat exchangers, underground disposal of radioactive waste materials, storage of foodstuff, exothermic chemical reactions in packed-bed reactor, crystal growth techniques, such as semiconductors crystal growth and alloys solidifications, where temperature and concentration differences are combined [1-4]. Furthermore, porous medium saturated with an electrically conducting fluid under a magnetic field has been the subject of numerous recent studies owing to the implication of the phenomenon in many engineering applications including cooling of electronic equipment, geothermal reservoir, solar energy collection, and crystal growth in liquids, metallurgical applications involving continuous casting and

* Corresponding authors, e-mails: hadd71@yahoo.fr

solidification of metal alloys and others [5, 6]. The double diffusive natural convection carried out in a 2-D cavity filled with a binary fluid and subjected to horizontal temperature and concentration gradients with cooperating volume forces has been analyzed by Gobin and Bennacer [7]. They have found that for a high value of Lewis number, the thermal transfer rate decreases as the buoyancy ratio increases. Numerical and a scale analysis were used to characterize the effect of the permeability ratio and the different governing parameters on the heat and mass transfer in bi-layered porous cavity. The results were presented in terms of streamlines, isotherms, iso-concentrations lines and for the average Nusselt, Nu_m, and Sherwood, Sh_m, numbers, and analyzed by Hadidi *et al.* [8, 9]. Recently, the natural convection induced by different wall boundary conditions in vertical and horizontal porous cavities filled with a binary fluid using the Dupuit-Darcy model has been studied analytically and numerically have been analyzed by Rebhi *et al.* [10, 11], characterizing the transition from a convective steady-state to oscillatory state. Corcione *et al.* [12] investigated numerically a double-diffusive natural convection in a vertical square enclosures induced by opposite horizontal temperature and concentration gradients. It was found that both heat and mass transfer increases as the thermal Rayleigh and Prandtl numbers were increased. Similarly, many researchers have investigated the effect of the presence of a magnetic field on double diffusive convection within square or rectangular cavities. We can mention here some studies as an example. Pirmohammadi and Ghassemi [13] investigated numerically the effect of a magnetic field on the laminar natural convection flows in a tilted enclosure filled with gallium liquid, which heated from below and cooled from the top while other walls were adiabatic. Sivasankaran and Bhuvaneswari [14] analyzed the effect of the magnetic field and aspect ratio on convective flow and heat transfer in a rectangular enclosure with partially thermally active vertical walls. Nine different relative positions of the thermally active zones are considered. The authors found that the flow field is altered when changing the direction of the magnetic field in the presence of strong magnetic field and the Nu_m decreases with an increase of the Hartmann number and increases with increase of the Grashof number and aspect ratio. Sarris *et al.* [15] presented a numerical study of unsteady 2-D natural convection in a laterally and volumetrically heated square cavity, filled with a liquid-metal under the influence of a magnetic field. The authors found that in the presence of a magnetic field, the flow dynamics as well as the rate of heat and mass transfer were considerably affected. Costa *et al.* [16] reported a numerical study of the effects of a magnetic field upon natural convection of electrically conducting fluids contained in differentially heated square enclosures filled with fluid-saturated porous media. The Darcy flow model was used for this investigation to describe the fluid-flow inside the fluid-saturated porous media. Grosan *et al.* [17] presented a numerical investigation of the steady MHD free convection in a rectangular cavity filled with a fluid-saturated porous medium and with internal heat generation where an inclined uniform magnetic field was externally imposed. Revnic *et al.* [18] investigated numerically the effects of an inclined magnetic field and heat generation on unsteady free convection within a square cavity filled with a fluid-saturated porous medium. The Darcy model was used for the mathematical formulation of the fluid-flow into porous media. The finite volume method has been used to solve the governing equations for heat and mass transfer.

To our knowledge, the uniform and tilted magnetic field and the inertial parameter effects on double diffusive convection across an inclined square porous cavity saturated by an electrically conducting binary mixture, with the use of Dupuit-Darcy flow model, has not been addressed and most of studies only deal with either the magnetic field effect or the inertia effect most studies on natural convection in porous medium for different configurations with the use of Darcy or Brinkman-extended Darcy's model. Since the emersion of the Dupuit-Darcy law,

a significant progress was made in designing high performance thermal systems where thermal convection is encountered. Therefore, the purpose of the present work is to investigate the double diffusive natural convection in an inclined porous a square cavity saturated with an electrically conducting binary mixture, in the presence of a constant tilted magnetic field and the Dupuit-Darcy model is used. The complete system of governing equations is solved numerically using the finite difference method. The main objective of the present investigation focuses on the examination of the combined effects of a uniform tilted magnetic field and inertia on double diffusive natural convection, the fluid-flow intensity, the heat and mass transfer for a wide range of the governing parameters.

Mathematical formulation of the problem

The physical configuration considered in this study is a square porous layer shown in fig. 1. The upper and bottom active walls are exposed to a constant and uniform temperatures and concentrations, respectively, while the lateral active walls are impermeable and adiabatic. The enclosure is filled with homogeneous porous medium saturated by Newtonian and electrically conducting fluid which is permeated by a uniform magnetic field, $\vec{B}_0$, with magnitude proportional to Hartmann number at an inclined angle, Φ, from the horizontal plane. Both the viscous dissipation and magnetic dissipation are assumed to be negligible.

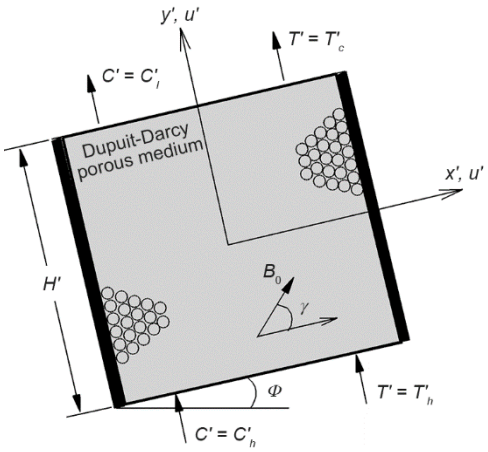

Figure 1. The physical model and co-ordinate system

The governing equations that describe the convective behavior of the system are conservation of the mass, momentum, energy and species, stated as flows using the conservative form assuming incompressible flow:

$$\frac{\partial u'}{\partial x'} + \frac{\partial v'}{\partial y'} = 0 \tag{1}$$

$$\frac{K}{\mu}\left\{-\frac{\partial p'}{\partial x'} + \rho g[\beta_T(T'-T_0') + \beta_C(C'-C_0')]\cos\Phi\right\} = \left(1 + \frac{\tilde{K}}{\mu}\rho\left|\vec{V}'\right|\right)u' + \vec{J}'\times\vec{B}_0' \tag{2}$$

$$\frac{K}{\mu}\left\{-\frac{\partial p'}{\partial y'} + \rho g[\beta_T(T'-T_0') + \beta_C(C'-C_0')]\sin\Phi\right\} = \left(1 + \frac{\tilde{K}}{\mu}\rho\left|\vec{V}'\right|\right)v' + \vec{J}'\times\vec{B}_0' \tag{3}$$

$$(\rho C)_p\frac{\partial T'}{\partial t'} + (\rho C)_f\left(u'\frac{\partial T'}{\partial x} + v'\frac{\partial T'}{\partial y'}\right) = k\nabla^2 T' \tag{4}$$

$$\phi\frac{\partial C'}{\partial t} + \left(u'\frac{\partial C'}{\partial x'} + v'\frac{\partial C'}{\partial y'}\right) = D\nabla^2 C' \tag{5}$$

$$\nabla\vec{J}', \quad \vec{J}' = \kappa(-\nabla\Phi' + \vec{V}'\times\vec{B}_0') \tag{6}$$

where u', v', p', g, μ, k, D, K, and $\tilde{K}$ stand for the velocity components of velocity $\vec{V}'$ in x'- and y'-directions, pressure, gravitational acceleration, dynamic viscosity, thermal conductivity of the saturated porous medium, mass diffusivity of species through the fluid saturated porous medium, medium permeability, and material parameter, respectively. To illustrate how the additional non-linear term comes into play when the porosity is high, we may quote Ergun's [19] relations for K and $\tilde{K}$ are given by: $K = d^2\varepsilon^3/150(1-\varepsilon)^2$ and $\tilde{K} = 1.75d^2/150(1-\varepsilon)$ in which ε denotes porosity and d – the characteristic pore or particle diameter. To reduce the number of unknowns, a stream-function, ψ', is introduced such that the continuity equation is satisfied by the following relationships:

$$u' = \frac{\partial \psi'}{\partial y'}, \quad v' = -\frac{\partial \psi'}{\partial x'} \tag{7}$$

The following dimensionless variables (primed quantities are dimensional) are used:

$$(x, y) = \frac{(x', y')}{H'}, \quad (u, v) = \frac{(u', v')H'}{\alpha}, \quad t = \frac{t'\alpha}{\sigma H'^2}, \quad p = \frac{p'K}{\mu\alpha}, \quad \theta_T = \frac{T' - T_0'}{T_\mathrm{h}' - T_\mathrm{c}'},$$

$$\theta_S = \frac{C' - C_0'}{C_\mathrm{h}' - C_\mathrm{l}'}, \quad \psi = \frac{\psi'}{\alpha}, \quad \varepsilon = \frac{\phi}{\sigma}$$

The dimensionless governing equations in terms of stream-function, temperature and concentration are then given first by the Dupuit-Darcy law for motion:

$$\mathcal{A}_x \frac{\partial^2 \psi}{\partial x^2} + \mathcal{A}_y \frac{\partial^2 \psi}{\partial y^2} + \mathcal{A}_{xy} \frac{\partial^2 \psi}{\partial x \partial y} = -\mathrm{Ra} \frac{\partial}{\partial x}(\theta_\mathrm{T} - \varphi\theta_\mathrm{S})\cos\Phi - \mathrm{Ra} \frac{\partial}{\partial y}(\theta_\mathrm{T} - \varphi\theta_\mathrm{S})\sin\Phi \tag{8}$$

The energy conservation equation as:

$$\frac{\partial \theta_\mathrm{T}}{\partial t} + \frac{\partial \psi}{\partial y}\frac{\partial \theta_\mathrm{T}}{\partial x} - \frac{\partial \psi}{\partial x}\frac{\partial \theta_\mathrm{T}}{\partial y} = \frac{\partial^2 \theta_\mathrm{T}}{\partial x^2} + \frac{\partial^2 \theta_\mathrm{T}}{\partial y^2} \tag{9}$$

and then by the mass conservation equation:

$$\varepsilon \frac{\partial \theta_\mathrm{S}}{\partial t} + \frac{\partial \psi}{\partial y}\frac{\partial \theta_\mathrm{S}}{\partial x} - \frac{\partial \psi}{\partial x}\frac{\partial \theta_\mathrm{S}}{\partial y} = \mathrm{Le}^{-1}\left(\frac{\partial^2 \theta_\mathrm{S}}{\partial x^2} + \frac{\partial^2 \theta_\mathrm{S}}{\partial y^2}\right) \tag{10}$$

with $\mathcal{A}_x, \mathcal{A}_x$, and $\mathcal{A}_{xy}$, are given, respectively, by:

$$\mathcal{A}_x = 1 + GQ + \left(\frac{\partial \psi}{\partial x}\right)^2 + \mathrm{Ha}^2 \sin^2 \Phi, \quad \mathcal{A}_y = 1 + GQ + \left(\frac{\partial \psi}{\partial y}\right)^2 + \mathrm{Ha}^2 \cos^2 \Phi,$$

$$\mathcal{A}_{xy} = 2\frac{\partial \psi}{\partial x}\frac{\partial \psi}{\partial y} GQ^{-1} + \mathrm{Ha}^2 \sin 2\Phi, \quad Q = \left[\left(\frac{\partial \psi}{\partial x}\right)^2 + \left(\frac{\partial \psi}{\partial y}\right)^2\right]^{1/2} \tag{11}$$

where θ_T and θ_S are the dimensionless temperature and concentration. The setting in no dimensional from of the governing equations gave rise to a group of dimensionless parameters, namely

the thermal Rayleigh number, the parameter that measures the inertial effects, G, the Hartmann number, the Lewis number, the buoyancy ratio, and the normalized porosity, defined as:

$$\mathrm{Ra}=\frac{\mathrm{g}K\beta_{\mathrm{T}}\Delta T'H'}{\alpha\nu},\quad G=\frac{\tilde{K}\alpha}{\nu H'},\quad \mathrm{Ha}=B_0\sqrt{\frac{\kappa K}{\mu}},\quad \mathrm{Le}=\frac{\alpha}{D},\quad \varphi=\frac{\beta_C\Delta S'}{\beta_{\mathrm{T}}\Delta T'},\quad \varepsilon=\frac{\phi}{\sigma}\tag{12}$$

Numerical method

The solution of the governing eqs. (8)-(10) is obtained using a finite difference method with uniform grid size. The energy and species, eqs. (9) and (10) were solved using an alternating-direction implicit method. The values of the time step were varied between 10^{-2} and 10^{-4} depending on the values of governing parameters. At each new time step, the SOR iterative procedure was repeated until the following criteria of convergence was fulfilled:

$$\frac{\sum_i\sum_j\left|\phi_{i,j}^{k+1}-\phi_{i,j}^{k}\right|}{\sum_i\sum_j\left|\phi_{i,j}^{k+1}\right|}\le 10^{-6}$$

where $\phi_{i,j}^{k}$, is the stream function value at the node (i, j) at the iteration, k^t. A further decrease of the convergence criteria below 10^{-6} does not cause any significant change in the final results. The validation of the numerical code has been performed over a large range of parameters. Some comparison results with Saeid and Pop [20] are presented in tab. 1. The results indicate that the agreement between the two numerical codes is excellent for the prediction of the strength of convection, $\psi_{\max}$, and the $\mathrm{Nu_m}$.

Table 1. Comparisons of $\psi_{\max}$ and $\mathrm{Nu_m}$ obtained from present code and the results presented in [20] for A = 1, Ra = 10^3, Ha = 0, φ = 0, and Φ = 90°

	[20]		Present study	
G	$\psi_{\max}$	$\mathrm{Nu_m}$	$\psi_{\max}$	$\mathrm{Nu_m}$
0	20.435	13.533	20.374	13.585
10^{-1}	7.995	4.747	8.054	4.841
10^{0}	4.045	2.375	4.106	2.433
10^{1}	1.650	1.295	1.744	1.322

Results and discussion

The purpose of the present study is to analyze the magnetic field and the inertial effects on the convective flow, the heat and mass transfer rates. In this section, both the flow structure and the heat transfer *vs.* the controlling parameters will be analyzed and discussed. Initially in this section we presented the numerical results obtained for Ra = 500, Le = 5, φ = –0.1, and γ = 90°. The numerical results reported in this study cover the range $0 \le G \le 10^4$, $0 \le \mathrm{Ha} \le 10$, $0 \le \mathrm{Ha} \le 500$, $0 \le \Phi \le 180°$, $0 \le \gamma \le 180°$, and $-5 \le \varphi \le 5$.

The streamlines, isotherms and iso-concentration lines are displayed in figs. 2-5 for Ra = 500, Le = 5, φ = –0.1, and different value of inertial parameter, G (0.1 and 10), magnetic field, Ha (0 and 10), inclination angle of the enclosure, Φ (45° and 135°), tilting angle of the magnetic field, γ (0° and 90°), are illustrated from left to right, respectively. The effect of G is depicted in figs. 2(a) and 2(b). The flow structure consists of a unicellular diagonal cell filling the entire cavity. The direction of the fluid circulation, which can be either clockwise or counter-clockwise, is induced by the round-off generated in the numerical computation. The increasing of inertial parameter form G = 0.1 to G = 10 reduces considerably the strength of the convective motion in the porous layer as indicated by the value of stream function at the center of the cavity: ψ_0 = 7.983 for G = 0.1, and ψ_0 = 0.266 for G = 10, the isotherms and iso-concentration lines which are less distorted indicating that the heat and mass transfer tends to be diffusive.

Consequently, as it can be observed from fig. 2(b), both the temperature and the concentration gradients are considerably inhibited with an increase of G, tend to have parallel constant temperature and concentration lines, at which: $Nu_m = 3.240$ and $Sh_m = 7.384$ for $G = 0.1$, and $Nu_m = 1.007$, and $Sh_m = 1.170$ for $G = 10$.

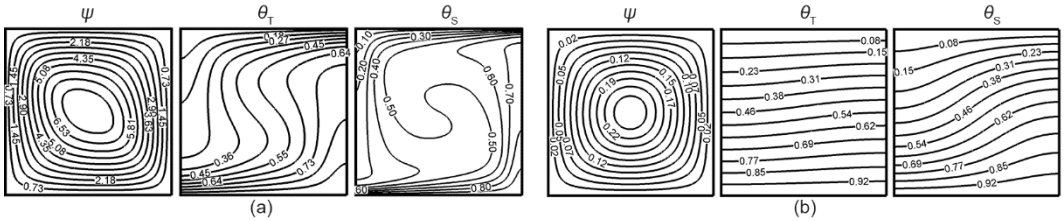

Figure 2. Contours of stream, temperature and concentration for Ha = 0, $\Phi = 0°$, and $\gamma = 90°$; (a) $G = 0.1$, $Nu_m = 3.222$, $Sh_m = 7.038$, (b) $G = 10$, $Nu_m = 1.007$, $Sh_m = 1.169$

The effects of the magnetic field on double-diffusive convection within a square cavity are illustrated in figs. 3(a) and 3(b) for Ha = 0 and Ha = 10 in the absence and presence of magnetic field. For this value, the resulting convection is relatively pronounced, as indicated by the value of $\psi_0 = 6.21$ and the more distortion of the temperature and concentration fields, $Nu_m = 3.688$ and $Sh_m = 9.820$. The retarding effect of the magnetic field is demonstrated in fig. 3(b) for Ha = 10. The result indicate that, for the set of governing parameters considered for this case, the convective circulation is progressively inhibited as the value of Hartmann number increased. For high value of Hartmann number (Ha = 10), the convective motion within the cavity is almost completely damped, $\psi_0 = 0.560$, by the magnetic field. As a result of the heat and mass transfer rates, $Nu_m = 1.074$ and $Sh_m = 2.071$, are almost purely conductive.

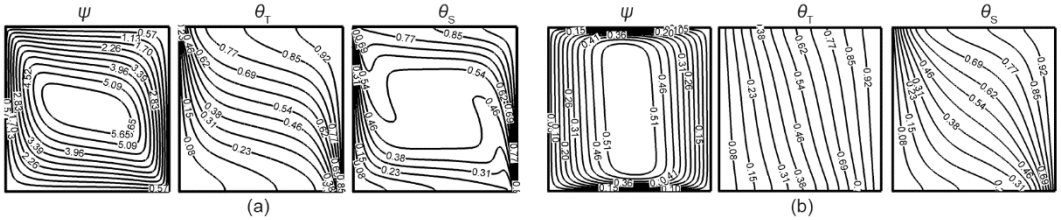

Figure 3. Contours of stream, temperature and concentration for $G = 0.1$, $\Phi = 90°$, and $\gamma = 90°$; (a) Ha = 0, $Nu_m = 2.668$, $Sh_m = 6.760$, (b) Ha = 10, $Nu_m = 1.036$, $Sh_m = 1.626$

Figures 4(a) and 4(b) depict streamlines, isotherms and iso-concentrations *vs.* inclination angle, Φ. It is clear from this figure that the convection effect increases for $\Phi = 45°$, which: $\psi_0 = 3.645$, $Nu_m = 2.031$, and $Sh_m = 5.323$ and decreases $\Phi = 135°$, which: $\psi_0 = 1.728$, $Nu_m = 1.401$, and $Sh_m = 4.046$. When the tilted angle over $\Phi = 135°$ eliminates convection effect, however the conduction heat and mass transfer becomes the dominant in this situation. Figures 5(a) and 5(b) exhibits the streamlines, isotherms and iso-concentration lines for Ha = 1, $G = 0$, $\Phi = 90°$, for different γ, equals to $\gamma = 0°$ and $\gamma = 90°$. As shown in figures previously mentioned, γ, the stream lines become weaker and the isotherms and iso-concentrations are more distorted for $\gamma = 90°$ at which: $\psi_0 = 11.022$, $Nu_m = 7.646$, and $Sh_m = 20.333$, which means that the natural convection becomes weak. While, the central stream line is elongated and the isotherms and iso-concentrations are less distorted for $\gamma = 0°$, at which: $\psi_0 = 9.895$, $Nu_m = 6.226$, and $Sh_m = 16.225$.

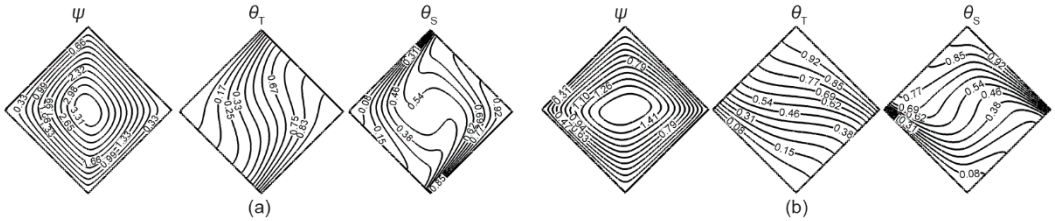

Figure 4. Contours of stream, temperature and concentration for G = 1, Ha = 1, γ = 90°; (a) Φ = 45°, Nu_m = 1.828, Sh_m = 4.466, (b) Φ = 135°, Nu_m = 1.233, Sh_m = 3.149

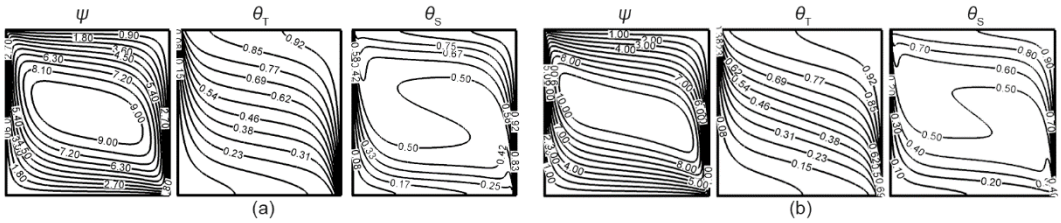

Figure 5. Contours of stream, temperature and concentration for G = 0, Ha = 1, Φ = 90°; (a) γ = 90°, Nu_m = 3.514, Sh_m = 9.603, (b) γ = 0°, Nu_m = 3.565, Sh_m = 11.097

Figure 6 shows the influence of Φ on the stream function amplitude at ψ_0, Nu_m, and Sh_m, respectively. The results are obtained for Ha = 1, γ = 90°, and different values of G. In the absence of inertial parameter (G = 0) the resulting curves are those corresponding to a porous medium modeled according to Darcy's law. The graphs clearly illustrate the fact that the Φ has a dominant effect on the strength of convection and the resulting heat and mass transfer. It is observed that, as the angle of inclination decreases from 180° to 0°, the Nu_m and Sh_m first increase, reaches a peak at $\Phi \approx 60°$ and then decrease.The effect of G on the stream function amplitude at the ψ_0 and on the Nu_m and Sh_m is illustrated in figs. 6(a)-6(c). The results are obtained for values of the inertial parameter ranging between G = 0 and G = 10. In general, it is noticeable from fig. 6(a) that, for a given value of the Φ an increase in the inertial parameter reduces the strength of convective motion in the layer considerably. Consequently, as can be observed from figs. 6(b) and 6(c), both the heat and mass transfer rates are significantly inhibited with an increase of G.

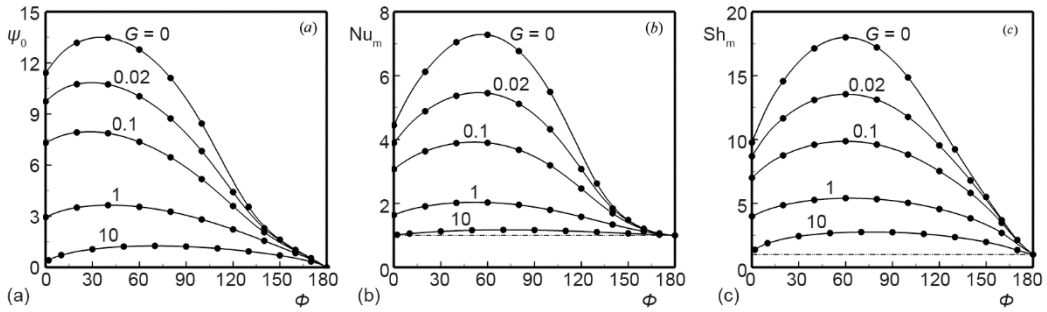

Figure 6. Effects of inclination angle, Φ, and inertial effects parameter, G, on ψ_0, Nu_m, and Sh_m

Figure 7 shows the evolution of ψ_0 and the average heat, Nu_m, and mass, Sh_m, transfer rates, respectively, as function of G for different values of Hartmann number, at Φ = 90° and

$\gamma = 90°$. A bird eye view of figs. 7(a)-7(c) reveals that, for small values of G, the strength of the convective motion and the heat and mass transfer rates increase sharply and tend asymptotically toward a constant value that depends on the Hartmann number. This limit presented for $G \to 0$ correspond to the pure Darcy flow regime. However, it is clear from figs. 7(a)-7(c) that, an increase of G annihilates the strength of the convection and the heat and mass transfer. In fact, for $G \to \infty$, the rest state is eventually reached, for which $\psi_0 \to 0$ and $Nu_m(Sh_m) \to 1$ and this independently of the value of the Hartmann number. On the other hand, the increasing effects of magnetic field on the ψ_0, Nu_m, and Sh_m are demonstrated in figs. 7(a)-7(c) for Hartmann number ranging between 0 and 6. An increase in Hartmann number reduces considerably the ψ_0, Nu_m, and Sh_m in the layer.

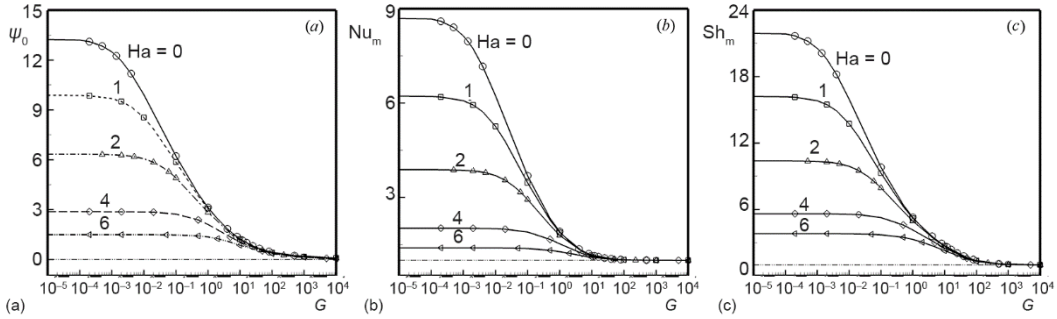

Figure 7. Effects of G and Ha for $\Phi = 90°$ and $\gamma = 90°$ on Nu_m and Sh_m

Figures 8(a)-8(c) show the variation of the ψ_0, Nu_m, and Sh_m with the Rayleigh number for Ha = 1, $\Phi = 90°$, $\gamma = 90°$ for different values of G. In general, it is seen from figs. 8(a)-8(c) that, increase in G leads to a decrease in both the strength of the circulation (the stream function), the Nu_m and Sh_m in the porous cavity. When $G = 10$, the Nu_m and Sh_m are approximately unity, $Nu_m(Sh_m) = 1$, and fig. 8(a) shows that the stream function is of the order of unity also for all the values of the Rayleigh number. It can be seen from figs. 8(a)-8(c) that increase in the inertial parameter leads to a slowdown in the double diffusive natural convection currents in the cavity and reduces the Nu_m and Sh_m for constant values of Rayleigh number. For low values of G, the Rayleigh number has more important effects on ψ_0, Nu_m, and Sh_m, than that at high values of inertial effects parameter G.

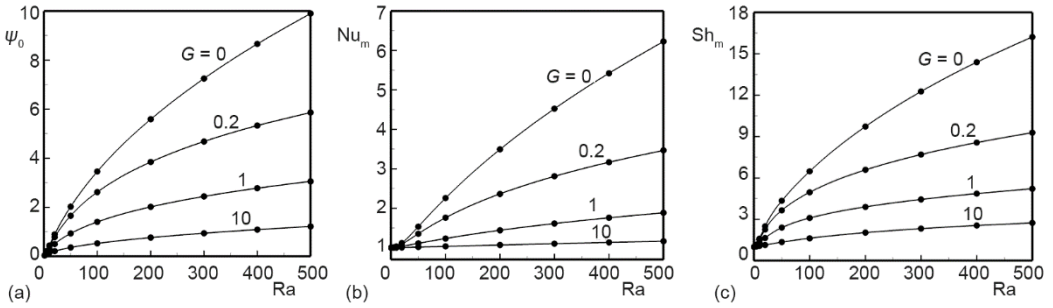

Figure 8. Variation of ψ_0, Nu_m, and Sh_m as a function of Ra for different values of G

Figures 9(a)-9(c) show typical bifurcation diagrams for ψ_0, Nu_m, and Sh_m as a function of Rayleigh and Hartman numbers for $G = 0.2$, $\Phi = 90°$ and $\gamma = 90°$. In the absence of a magnetic field (Ha = 0), the critical Rayleigh number for the onset of motion, is given by $Ra^{sup} \approx 0$, at

which convection occurs. In general, it is seen from figs. 9(a)-9(c) that, for a given Rayleigh number, an increase in the magnetic field reduces considerably both the strength of the circulation, ψ_0, and heat and mass transfer rates (Nu_m, and Sh_m).

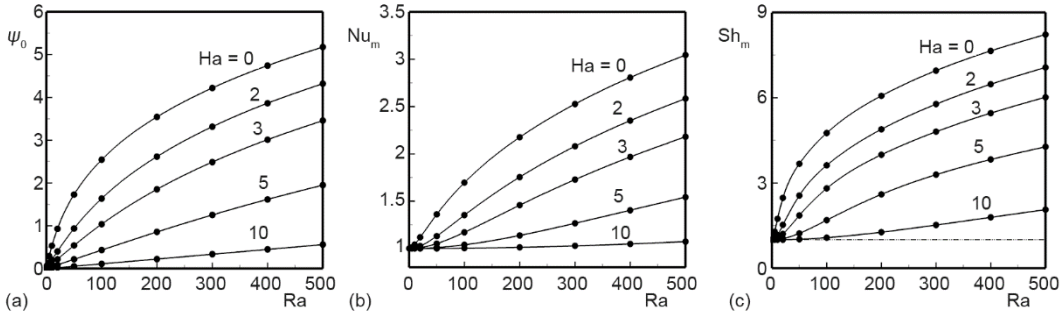

Figure 9. Bifurcation diagram as a function of Ra and Ha for G = 0.2, on Nu_m, and Sh_m

Figures. 10(a)-10(c) illustrate the influence of the buoyancy ratio, φ, on ψ_0, Nu_m, and Sh_m for Ha = 1, Le = 2, $\Phi = 90°$ and $\gamma = 90°$, and different values of G. The buoyancy ratio is varied in the range –5 to 5 for opposing flow, aiding flow and thermal driven flow ($\varphi < 0$, $\varphi > 0$, and $\varphi = 0$), *i. e.* this covers the range from aided solutal-dominated flow ($\varphi = 5$), to purely thermal-dominated flow ($\varphi = 0$), to opposed but solutal-dominated flow ($\varphi = –5$). For $\varphi = 0$ (absence of solute concentration effects) the convective motion is induced only by the temperature gradients, giving rise to counter-clockwise thermal circulation ($\psi_0 > 0$), see the streamlines in fig. 11(a). When φ is above zero, the thermal and solutal buoyancy forces act in the same direction and the anticlockwise convective flow ($\psi_0 > 0$) is considered to be aided. Figure 10(a) indicates that the flow behavior depends considerably upon whether the buoyancy ratio is below or above the critical buoyancy ratio, $\varphi_{cr} = –1$, for this value $\varphi_{cr} = –1$ the thermal effects are still predominant such that ψ_0 is positive (zero) provided that $\varphi = \varphi_{cr}$. When φ is below zero, the thermal and solutal buoyancy forces are now opposing each other. For low negative values of φ the flow is again dominated by the mass species *i. e.* (solutally dominated) the flow circulation is now clockwise) ($\psi_0 < 0$), see the streamlines in fig. 11(b). It is interesting to observe from these figures the existence of minimum values in both Nu_m and Sh_m for a buoyancy ratio of about $\varphi = –1$. The values of flow intensity ψ_0, Nu_m, and Sh_m tend to increase with increasing the absolute values of φ for all the values that we studied. It is observed that both the strength of fluid circulation, Nu_m and Sh_m decrease with an increase in the inertial effects parameter.

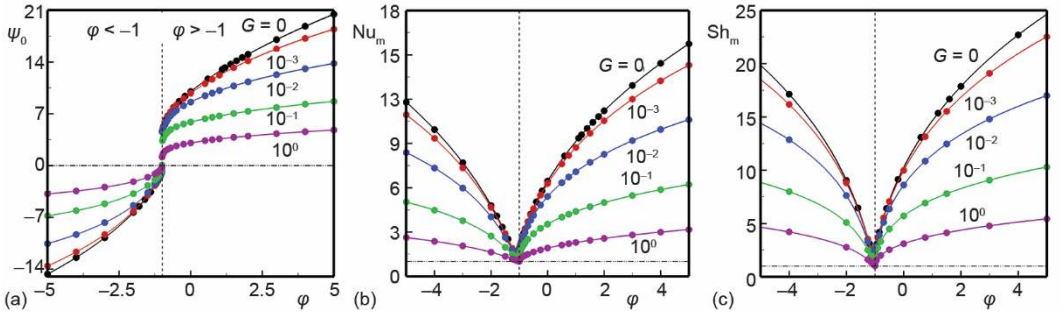

Figure 10. Effects of G and φ for Le = 2, $\Phi = 90°$, $\gamma = 90°$ on ψ_0, (b) Nu_m, and (c) Sh_m
(*for color image see journal web site*)

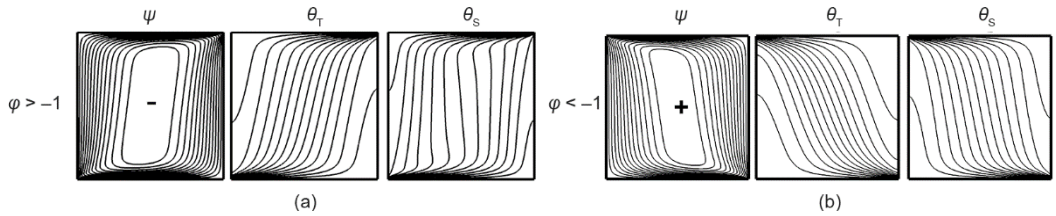

Figure 11. Streamlines, isotherms and iso-concentrations from clockwise ($\varphi > -1$) to counterclockwise ($\varphi < -1$) for $G = 10^{-2}$, Le = 2, $\Phi = 90°$, $\gamma = 90°$; (a) $\varphi = 3$, (b) $\varphi = -3$

The magnetic effect, Ha, on the ψ_0, Nu_m, and Sh_m for *vs.* φ is depicted in fig. 12.

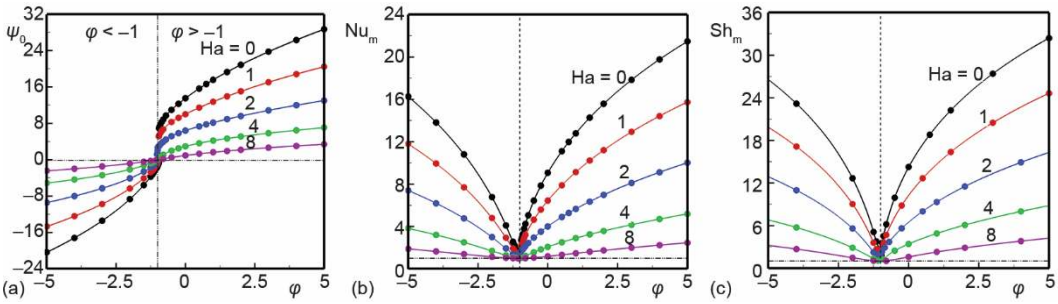

Figure 12. Effects of Ha and φ for Le = 2, $\Phi = 90°$, $\gamma = 90°$ on ψ_0, Nu_m, and Sh_m
(*for color image see journal web site*)

The variation of ψ_0, Nu_m, and Sh_m with G for different values of Φ for Ha = 1 and $\gamma = 90°$ is presented in figs. 13(a)-13(c).The results indicate that the maximum of ψ_0, Nu_m, and Sh_m is obtained when $\Phi = 45°$. At very large values of Φ ($\Phi = 180°$), the heat and mass transfer become primarily conductive such that ψ_0, Nu_m, and Sh_m remain constant independently of the value of G. Naturally, as illustrated in figs.13(a)-13(c), the increase of inertial effects parameter reduces the strength of the convective heat and mass transfer such that eventually, $\psi_0 \to 0$ and $Nu_m(Sh_m) \to 1$, and this independently of Φ of the cavity.

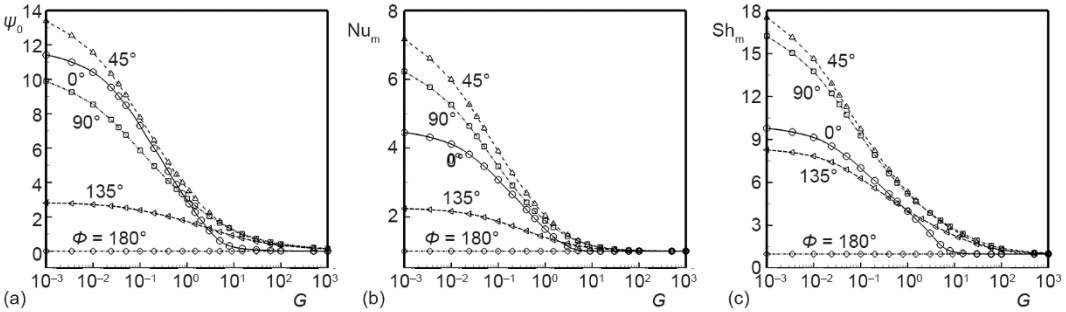

Figure 13. Effects of G and Φ for Ha = 1, Le = 5, $\gamma = 90°$ on ψ_0, Nu_m, and Sh_m

Figure 14 shows the effect of the inclination angle of the magnetic field about the horizontal direction, γ, on the Nu_m and Sh_m, respectively for $G = 1$, Ha = 1, and $\Phi = 90°$. The optimal heat and mass transfer rates appear when the magnetic field becomes horizontal, $\gamma = 0°$.

A bird eye view on the graphs indicates that, 3.867(11.225) and 3.395(8.991) in the average heat and mass transfer rates, $Nu_m(Sh_m)$, was recorded between the two inclinations, $\gamma = 90°$ and $\gamma = 0°$. A 12.2% (19.9%) rise in the $Nu_m(Sh_m)$ was recorded between the two inclinations, $\gamma = 0°$ and $\gamma = 90°$. In addition, this trend demonstrates the robustness of the numerical method to take into account the orientation of the magnetic field, which is the reason why the study has been restricted to orientations of the prime quadrant.

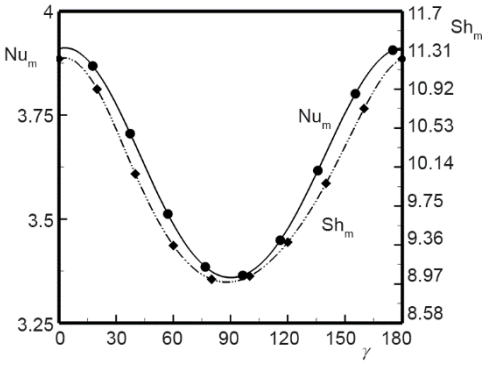

Figure 14. Variation of Nu_m and Sh_m *vs.* the inclination angle in the range from $\gamma = 0°$ to $\gamma = 180°$ for Ra = 500, G = 1, Ha = 1, and $\Phi = 90°$

Conclusion

The present study showed that the convective motion and the heat and mass transfer rates were rather very sensitive to the inertial and magnetic field parameters. It is found that, for a set of governing parameters, Ra, Le, Φ, φ, and γ, the strength of the circulation, ψ_0, the resulting heat transfer, Nu_m, and mass transfer, Sh_m, decrease with an increase in the inertial effects and the magnetic field parameters. In fact, for $G \gg 1$ (Ha $\gg 1$), the rest state is eventually reached, for which the heat and mass transfer were ruled mostly by conduction, *i. e.*, $\psi_0 = 0$ and $Nu_m(Sh_m) = 1$. The orientation of the layer has a large effect on the convective heat and mass transfer. Independently of the value of the inertial effects parameter, the maximum heat and mass transfer rates occur when the layer is heated and salted form the bottom. For a given values of Ra, Le, Φ, φ, and γ, the peaks of the Nu_m and Sh_m occur at given angles Φ_m that depends considerably upon G. In addition, it was predicted that an increase of the inertial (magnetic field) effects parameter, G(Ha), does not affect the threshold for the onset of convection, $Ra_C^{sup} \approx 0$, since this latter occurs at the rest state ($\psi_0 = 0$). Thus, as the buoyancy ratio parameter increases above $\varphi > \varphi_{cr}$, the strength of the convective motion increases. An optimal heat and mass transfer rates appears when the magnetic field becomes horizontal $\gamma = 0°$. A 12.2% (19.9%) rise in $Nu_m(Sh_m)$ was recorded between the two inclinations, $\gamma = 0°$ and $\gamma = 90°$.

Nomenclature

$\vec{B}'_0$ – applied magnetic field, [Vsm^{-2}]
D – mass diffusivity of species, [m^{2}s^{-1}]
G – inertial effects parameter, $(= \tilde{K}\alpha/\nu H')$
g – gravitational acceleration, [ms^{-1}]
H' – enclosure height, width, [m]
Ha – Hartmann number, $(= B_0\sqrt{kK/\mu})$
K – permeability of the porous medium, [m^2]
k – thermal conductivity, [Wm^{-1}K^{-1}]
L' – width of the enclosure, [m]
Le – Lewis number, $(= \alpha/D)$
Ra – thermal Rayleigh number, $(= g\beta_T K\Delta T'H'/\alpha\nu)$
S' – dimensionless concentration
$\Delta T'$ – temperature difference $(= T'_h - T'_c)$

Greek symbols

α – thermal diffusivity, [m^{2}s^{-1}]
β_S – species expansion coefficient
β_T – thermal expansion coefficient, [K^{-1}]
γ – tilting angle, [°]
κ – electrical conductivity, [Ω^{-1}m^{-1}]
μ – dynamic viscosity of fluid, [kgm^{-1}s^{-1}]
ν – kinematic viscosity, [m^{2}s^{-1}]
φ – buoyancy ratio, $(= \beta_S\Delta S'/\beta_T\Delta T')$
Φ' – electric potential

Subscript

0 – refers to the value taken at the center of the cavity

Superscript

′ – refers to dimensional variable

References

[1] Beghein, C., *et al.*, Numerical Study of Double-Diffusive Natural Convection in a Square Cavity, *Int. J. Heat Mass Tran.*, *35* (1992), 4, pp. 833-846
[2] Teamah, M. A., *et al.*, Numerical Simulation of Double-Diffusive Natural Convective Flow in an Inclined Rectangular Enclosure in the Presence of Magnetic Field and Heat Source, *Int. J. Ther. Sci.*, *52* (2012), 4, pp. 161-175
[3] Marina S. A., *et al.*, Effect of Thermal Radiation on Natural Convection in a Square Porous Cavity Filled with a Fluid of Temperature-Dependent Viscosity, *Thermal Science, 22* (2018), 1B, pp. 391-399
[4] Sivanandam, S., *et al.*, Natural Convection in an Inclined Porous Triangular Enclosure with Various Thermal Boundary Conditions, *Thermal Science, 23* (2019), 2A, pp. 537-548
[5] Jana, S., *et al.*, A Numerical Simulation Study for the Czochralski Growth Process of Si Under Magnetic Field*, Int. J. of Eng. Sci*., *44* (2006), 8-9, pp. 554-573
[6] Mariani, V., Moura Belo, I., Numerical Studies of Natural Convection in a Square Enclosure, *Ther. Eng*., *5* (2006), 1, pp. 68-72
[7] Gobin, D., Bennacer, R., Cooperating Thermosolutal Convection in Enclosures II. Heat Transfer and Flow Structure, *Int. J. Heat Mass Trans.*, *39* (1996), 13, pp. 2683-2697
[8] Hadidi, N., *et al.*, Bi-Layered and Inclined Porous Collector: Optimum *Heat and Mass Transfer, Energy*., *51* (2013), Mar., pp. 422-430
[9] Hadidi, N., *et al.*, Two-Dimensional Thermosolutal Natural Convective Heat and Mass Transfer in a Bi-Layered and Inclined Porous Enclosure, *Energy*., *93, Part 2* (2015), Dec., pp. 2582-2592
[10] Rebhi, R., *et al.*, Form Drag Effect on the Onset of Non-Linear Convection and Hopf Bifurcation in Binary Fluid Saturating a Tall Porous Cavity, *Int. J. Heat. Mass. Trans.*, *100* (2016), Sept., pp. 178-190
[11] Rebhi, R., *et al.*, Bistability and Hysteresis Induced by Form Drag in Nonlinear Subcritical and Supercritical Double-Diffusive Lapwood Convection in Shallow Porous Enclosures, *J. Fluid. Mech*., *812* (2017), Feb., pp. 463-500
[12] Corcione, M., *et al.*, Correlations for the Double-Diffusive Natural Convection in Square Enclosures Induced by Opposite Temperature and Concentration Gradients, *Int. J. Heat Mass Trans.*, *81* (2015), Feb., pp. 811-819
[13] Pirmohammadi, M., Ghassemi, M., Effect of Magnetic Field on Convection Heat Transfer Inside a Tilted Square Enclosure, *Int. Comm. Heat Mass Trans.*, *36* (2009), 7, pp. 776-780
[14] Sivanandam, S., Marimuthu, B., Effect of Thermally Active Zones and Direction of Magnetic Field on Hydromagnetic Convection in an Enclosure, *Thermal Science, 15* (2011), Suppl. 2, pp. S367-S382
[15] Sarris, I. E., *et al.*, MHD Natural Convection in a Laterally and Volumetrically Heated Square Cavity, *Int. J. Heat Mass Trans.*, *48* (2005), 16, pp. 3443-3453
[16] Costa, V. A. F., *et al.*, Natural Convection in Square Enclosures Filled with Fluid-Saturated Porous Media Under the Influence of the Magnetic Field Induced by Two Parallel Vertical Electric Currents, *Int. J. Heat Mass Trans.*, *55* (2012), 23-24, pp. 7321-7329
[17] Grosan, T., *et al.*, Magnetic Field and Internal Heat Generation Effects on the Free Convection in a Rectangular Cavity Filled with a Porous Medium, *Int. J. Heat Mass Trans.*, *52* (2009), 5-6, pp. 1525-1533
[18] Revnic, C., *et al.*, Magnetic Field Effect on the Unsteady Free Convection Flow in a Square Cavity Filled with a Porous Medium with a Constant Heat Generation, *Int. J. Heat Mass Trans.*, *54* (2011), 9-10, pp. 1734-1742
[19] Ergun, S., Fluid Flow Through Packed Columns, *Chem. Eng. Prog.*, *48* (1952), Feb., pp. 89-94
[20] Saeid, N. H., Pop, I., Non-Darcy Natural Convection in a Square Cavity Filled with a Porous Medium, *Fluid. Dynams. Res*., *36* (2005), 1, pp. 35-43

Paper submitted: January 17, 2019
Paper revised: May 3, 2019
Paper accepted: May 21, 2019